Marine vessel wave wake: transient effects when accelerating or decelerating

G.J. Macfarlane[1] and K.J. Graham-Parker[2]

1 Ph.D., M.Phil., B.Eng, Associate Professor and Manager Towing Tank & Model Test Basin, gregorm@amc.edu.au, Locked Bag 1395, Australian Maritime College, University of Tasmania, Launceston, Tasmania, 7250, Australia

2 B.Eng. Research Engineer, kjparker@live.com.au, Locked Bag 1395, Australian Maritime College, University of Tasmania, Launceston, Tasmania, 7250, Australia

ABSTRACT

It is well known that the waves generated by marine vessels, often referred to as wave wake or wash, can cause many issues when operating in sheltered waterways. This includes, but is not limited to; erosion of shorelines, damage to maritime structures and present a danger to other waterway users. Much research has been undertaken to better understand the characteristics of these waves and their effects, especially for high speed vessels that operate in shallow water where particularly large and energetic waves are generated. However, virtually all previous studies have generally only considered steady state conditions where vessel speed remains constant. There are many vessel operations, particularly commuter ferries, where regular passages through the trans-critical zone to super-critical speeds (in terms of depth Froude number) are required. The present study has performed a novel series of model scale experiments to quantify the waves during both acceleration and deceleration phases. Notable transient effects occur during the acceleration phase that significantly increase both the height and period of the maximum wave when compared to those at the corresponding steady-state speed. It is the wave characteristics at constant speed that are used when assessing whether a particular vessel meets wash criteria, thus it is quite likely that such criteria are significantly exceeded when a vessel accelerates to a super-critical speed, which could lead to the occurrence of the aforementioned wave wake issues. Interestingly, the study has also found that there is no such increase in wave characteristics when the same vessel decelerates back through the trans-critical speed zone.

KEYWORDS

Wave wake, wash, depth Froude number, acceleration, deceleration, ferry operations, variable Froude number, experiments.

INTRODUCTION

General Background

Whenever a body moves through water, such as a boat or ship, a pattern of waves is developed. The basic form of the wave pattern is primarily dependant on the vessel's speed and the water depth it is travelling, as governed by the depth Froude number (Equation 1).

$$Fr_h = \frac{u}{\sqrt{gh}} \qquad \text{Equation 1}$$

Speeds identified with a Fr_h of less than approximately 0.7 are known as sub-critical and indicate the area where the well-known Kelvin deep water wave pattern is formed, as depicted in Figure 1 (far left) and explained by Thomson (1887). When approaching the critical speed ($Fr_h = 1.0$) a vessel operates in the trans-critical zone (approximately $0.7 < Fr_h < 1.0$). At the depth critical speed, large transverse waves with crests orthogonal to the direction of the vessel are produced. When a vessel operates in the super-critical region, where Fr_h is greater than 1.0, the waves become long-crested in contrast to the shorter-crested waves of the sub-critical wave pattern and transverse waves are no longer produced because of the depth-limited wave speed. Each of the wave pattern regimes are illustrated in simplistic form in Figure 1.

Travelling at or close to critical speed is accompanied by a peak in wave-making resistance, sinkage and trim. If a vessel is travelling close to the critical Froude depth number in a laterally bounded waterway, such as a canal or channel, the perpendicular wave crest cannot grow laterally and the restrained energy disperses ahead of the vessel periodically in the form of two-dimensional waves known as solitons (Ertekin et al. 1984). In such cases the critical speed was known to occur at a Froude depth number below 1.0. A significant amount of research has focused on the growth of non-linear waves generated in the critical regime, for example: Grue, 2017; Soomere, 2007; Lee & Grimshaw, 1990; Akylas et al., 1988; Wu, 1987; Ertekin et al., 1986.

Wave Wake Issues

Since the 1980s the wave wake generated by high-speed marine vessels has seen a variety of new issues arise for other users of a waterway and the surrounding environment (PIANC 2003; Murphy et al. 2006). These include:

- shoreline (or bank) erosion and/or accretion;
- damage or nuisance to moored vessels;
- damage to jetties and other marine structures;

- endangering people working or enjoying activities in small craft or close to the shore;
- destruction of fragile water plants;
- disturbance of silt;
- damage to the ecology of intertidal and shallow sub-tidal habitat.

The waves generated by large high-speed craft have been blamed for causing several serious accidents, including some fatalities, as was experienced in a well-publicised incident in the United Kingdom in July 1999 where a shoaling wave from a 122 m long high-speed ferry grew to a reported 4 m in height close to shore, swamping a recreational fishing vessel and drowning one person (Marine Accident Investigation Branch 2000).

Vessel wave wake has also contributed to a number of very costly failed vessel operations, primarily due to the vessels being forced to operate at speeds well below those in which they were designed in order to minimise wash, thus negating their intended speed advantage. Examples where these and similar issues have been experienced can be found in Australia (Macfarlane et al. 2008; 2014), British Columbia (The Vancouver Sun, 2009), New Zealand (Parnell et al. 2007), Denmark (Parnell and Kofoed-Hansen 2001), Puget Sound, USA (Stumbo et al. 1999), San Francisco Bay, USA (Austin 1999), Sweden (Strom and Ziegler 1998) and Estonia (Soomere 2005).

When assessing vessel wave wake, it is now widely accepted that both wave height and period are of equal importance. This is reflected in most wave wake regulatory criteria adopted these days which generally focus on these characteristics for at least one key wave.

High-Speed Vessel Operation

The Permanent International Association of Navigation Congresses (PIANC) coordinated a working group to develop guidelines for the effective management of wave wake from large high-speed vessels operating in coastal regions (PIANC 2003). They stated that the effective management of large high-speed vessel wave wake is a multi-faceted problem that defies a simple “one size fits all” solution and they encouraged waterway managers and high-speed vessel operators to follow the guidelines for conducting a route assessment to aid with the development of management measures. They recommend that operation at trans-critical depth Froude numbers between approximately 0.85 and 1.1 be avoided, and that it is desirable to pass through this near-critical speed range as quickly as possible.

The PIANC guidelines also raise two other key points that are very relevant to the present study. Firstly, when a vessel accelerates through the trans-critical range bound for a super-critical speed, even if the operator recognises that unacceptable waves are being generated when the vessel is abeam of a sensitive location and reduces speed immediately,

it is likely that substantial wash would still propagate to that location due to the propagating angle of the waves. Therefore, it is important to recognise that the wash progressing toward the shoreline may have been caused by operating at or near-critical speed during a previous part of the passage. The guidelines also pointed out that a high-speed vessel could continue to operate at constant speed but the wash regime could change with variation of water depth along the vessel route. For example, a vessel could operate at a high speed in deep water at a sub-critical depth Froude number as it approaches shallower water. Continued operation at a high speed into shallow water results in the transition to critical speed, and potentially to super-critical speeds, depending on the bathymetry.

Feldtmann and Garner (1999) suggest that by using the depth Froude number and intelligent use of existing bathymetry and speed selection the effects of large waves created by high-speed vessels can be reduced by minimising the time taken to transition from sub- to super-critical speeds, or vice versa. In situations for which the bathymetry was not conducive to achieve this speed transition, they suggested a *critical speed step* could be created, in which the water depth along the vessel route could be deliberately altered to suit the operations.

Research into Variable Froude Number

Despite the acknowledgement that vessel operations through the trans-critical speed regime can raise significant concerns, there has been a distinct lack of targeted research to quantify the potential effects. To the authors' knowledge, virtually every published study that has attempted to quantify vessel generated waves in a systematic manner has only involved steady-state speeds – little or no consideration has been given to the acceleration or deceleration phases.

There are limited exceptions. Torsvik and Dysthe (2006) used numerical simulations based on Boussinesq equations to provide a more complete account of the processes which influence the wave pattern when a ship accelerates or decelerates while transitioning the critical speed region in a shallow channel. The authors first reviewed several other articles that have mathematically considered the effect of variable depth Froude number from which they observed that none give a comprehensive description of the wave pattern generated during the transition through the trans-critical speed region for a wide range of parameters. From their study, Torsvik et al. conclude when a vessel decelerates from super- to sub-critical speed it will always generate a solitary wave with significant amplitude, and that this amplitude becomes larger as the transition time increases, as this time allows the solitary wave to fully develop while in the upper part of the trans-critical region.

Torsvik and Dysthe (2006) also concluded that when a vessel accelerates from sub- to super-critical speed the amplitude of the solitary wave generated during this transition is highly dependent on the transition time. Their numerical simulations indicate that there is no solitary wave of appreciable amplitude for a fast transition, but as transition times

increase it will result in the generation of an upstream bore. The vessel is able to overtake the bore when the transition time is increased, subsequently reducing the bore amplitude and transforming into a solitary wave downstream. For long transition times, the amplitude of the upstream bore continues to grow until it is beyond the applicability of their model (thus producing unrealistic results).

Other investigations have indirectly considered the topic of wave patterns generated when a vessel accelerates or decelerates. For example, it is common for experiments to be performed in towing tanks to measure the wave pattern of a model ship from which the hull's wave resistance can be calculated (generally for predicting powering performance). It is usual for these analyses to be performed with the ship model at constant speed, however Wehausen (1961) recognised that initial acceleration is unavoidable in towing tanks, and that the waves created are different to those at steady-state speeds. He showed that the effect of this initial acceleration on wave resistance has a decaying and oscillating character. Calisal (1977) gave the general form of the initial acceleration potential and showed the existence of a two-dimensional wave. Calisal (1980) went on to perform a series of experiments to study the validity of the theoretical results. When the primary aim is to acquire steady-state data, Calisal concluded that the ship model should travel a distance proportional to the square of the Froude number before wave data collection should commence in order to avoid the effects from the initial acceleration waves. It was also noted that the proximity of the tank side walls is important and that it is expected that wider towing tanks (or basins) will experience reduced effects.

For the present study, the primary objective was to extend our knowledge on the typical magnitude of changes in wave characteristics when a vessel accelerates or decelerates through trans-critical speeds and consider the practical implications of these effects. Rather than focussing on the initial long period wave or possible solitons, this study places more emphasis on the height and period of the "maximum" wave within the entire wake (the individual wave possessing the greatest height), as this wave is almost always scrutinised when assessing compliance when wave wake regulations are imposed on a vessel/route. This was achieved by performing a systematic series of physical scale model experiments where the characteristics of the maximum waves are quantified for a wide range of typical acceleration and deceleration rates and compared against those for the corresponding constant speed. The present focus is on constant shallow depth, but relatively wide, waterways where no lateral restrictions/banks are present.

METHODOLOGY

A series of physical scale model experiments were performed in the 35 m long by 12 m wide shallow water basin at the Australian Maritime College, University of Tasmania. The water depth in the basin (h = 0.30 m) was set to a constant

finite value such that the vessel speeds investigated covered sub-critical, trans-critical and super-critical Froude depth numbers. Water surface elevations were acquired at many longitudinal locations at a fixed transverse distance from the sailing line of the ship model. Due to the potentially large number of variables involved, the size of the test program was limited to just a single hull form and two operational speeds. The four operational test scenarios are summarised as follows:

- Accelerate from stationary to a low super-critical speed (Fr_h = 1.17).
- Accelerate from stationary to a higher super-critical speed (Fr_h = 1.75).
- Decelerate from a low super-critical speed (Fr_h = 1.17) down to stationary.
- Decelerate from a higher super-critical speed (Fr_h = 1.75) down to stationary.

The body plan of the 1:20 scale model of a hard-chine planing monohull with nominal length L = 1.0 m used in these experiments is shown in Figure 2, while the principal particulars are provided in Table 1. The water depth to model length ratio remained constant at 0.30 for the entire series of tests, while the water depth to (static) draught ratio was 4.8. The model was fixed to an unmanned carriage that towed it in a straight and horizontal line with freedom in heave, trim, pitch and roll (constrained in surge, sway and yaw). This carriage runs along linear bearings fixed to a rigid truss that spans the length of the test basin. Measurement of the model speed was accomplished by logging the voltage output through a speed control unit linked to the electric drive motor. The measured speed was found to be very close to the tolerances recommended by the ITTC (2014), according to which the speed of the model was to be measured to within 0.1% of the maximum speed or to within 3 mm/s, whichever was larger.

A series of conventional two-wire resistance-type wave probes from HR Wallingford (Wallingford, United Kingdom) (each of length 300mm, accurate to approximately +/-0.25mm) were configured in both longitudinal and transverse arrays. The longitudinal array, positioned two boat-lengths from the sailing line of the model, consisted of eight equispaced probes and is of more relevance to the present study than the transverse array (which was used for a separate study into wave decay over distance). A plan view of the general layout of the facility and test apparatus is provided in Figure 3.

For the first phase of the test campaign, in which vessel acceleration was investigated, the model was accelerated at a constant rate from a stationary starting position 2.0 m before the first longitudinal wave probe (LWP1). After the desired speed had been reached, it remained constant until the model was well beyond the last longitudinal wave probe (LWP7) until the test was stopped. In the latter two phases of the test program, for which deceleration runs were conducted, the

model was rapidly accelerated so that it was running at a steady-state speed well before reaching the first probe in the longitudinal array. The deceleration phase began when the model was level with the LWP1 probe.

As explained in the first paragraph of this section, the first scenario simulated a case in which the critical depth Froude number was marginally exceeded (Fr_h = 1.17). The higher speed represented a well developed super-critical speed (Fr_h = 1.75). In each of the four scenarios, a total of seven different acceleration and deceleration rates were investigated, as detailed in Tables 2 and 3 respectively.

For the experiments investigating the effect of acceleration, the model commenced at x = 0 metres and was accelerated to the prescribed speed (e.g. Fr_h = 1.17) over the prescribed distance (e.g. 4 boat lengths), where the speed remained constant until the model passed the last longitudinal wave probe (LWP7), after which it was decelerated to a stop. For the deceleration experiments, the model was rapidly accelerated, held at the prescribed steady-state speed (e.g. Fr_h = 1.75), then commenced deceleration over the prescribed distance when in line with the first longitudinal wave probe (LWP1).

The eight wave probes that form the longitudinal array were spaced 2.0 m apart. In order to acquire a time-series record of the water surface elevation at many more probe positions, additional tests were performed with the starting position for the ship model offset. For example, for the acceleration tests at Fr_h of 1.17, the model start position was offset by -0.5 m, +0.5 m and +1.0 m from the nominal start position (a total of four runs, including the original run, were required for each acceleration rate), subsequently obtaining data at 32 different longitudinal locations at 0.5 m increments between 1.5 m and 17.0 m from the nominal model start position. For the deceleration tests the point at which deceleration commenced was offset by +1.0 m to obtain data at 16 different longitudinal locations at 1.0 m increments between 0 m and 15.0 m from commencement of deceleration. Both the probe location and maximum wave height are non-dimensionalised by dividing by model length.

RESULTS AND DISCUSSION

In virtually all previously known wave wake experiments the focus has been on quantifying the wave characteristics when all conditions remain constant – especially vessel speed and water depth. For the present study, our primary aim was to investigate the characteristics of the waves generated when the depth Froude number varied: first, when a vessel accelerates from a forward speed of zero to a specified steady-state speed, and second, when it decelerated from the steady-state speed back to a forward speed of zero. Particular interest is on the wave characteristics while Fr_h varies: are

there any transient effects such that the maximum wave height or its corresponding wave period exceed those at the steady-state speed?

In all of the cases investigated, it was observed during the experiments in the controlled environment that the wave pattern altered between the various general depictions provided in Figure 1. For example, in each case the typical Kelvin wave pattern was visible when the model was clearly operating at sub-critical speeds and, similarly, the longer-period super-critical wave pattern was quite obvious when operating well in excess of the critical speed. Due to the nature of the investigation, where speed was intentionally changing as the model passed (at various rates) through the trans-critical regime, it was difficult to clearly observe the 'classical' transverse-dominated wave pattern associated with operation at the critical speed, presumably due to insufficient time spent at or close to this speed.

A typical time series record of the water surface elevation from a single wave probe is presented in Figure 4 (from Run 137, $Fr_h = 1.75$, acceleration distance = 2 m, wave probe position = 8 m from model start position). The maximum wave is identified in this figure, including definitions of the maximum wave height (H_m) and period (T_m).

For each of the two steady-state speeds a total of seven different acceleration distances were investigated. To illustrate the analysis process, the resulting maximum wave heights at each of the 32 longitudinal locations (wave probes) from the model start position are plotted as a function of the non-dimensional distance from this start position for a single acceleration distance in Figure 5.

In the example shown in Figure 5, the dashed blue curve shows the model speed increasing from zero up to $Fr_h = 1.17$ over the distance of 10 boat lengths, after which the speed remains constant (the acceleration is constant while the velocity increases linearly and the model position is quadratic in time). The experimental points (green diamonds) indicate the non-dimensionalised maximum wave height at multiple locations along this acceleration distance and beyond. Unlike the speed, it is clear that this wave height does not increase linearly, but does reach a peak close to the point at which the steady-state speed is achieved.

The dashed grey line in Figure 5 indicates the non-dimensional maximum wave height for the steady-state speed (acquired from other runs). It can clearly be seen that a peak in maximum wave height occurs during the acceleration phase and that it is significantly larger than the steady state case. It can also be seen how the maximum wave height gradually decreases following this peak, until it approximately equals that of the steady-state case (as expected). The increase in maximum wave height is believed to be due to transient dynamic effects that occur while the model is accelerating, such as additional hull resistance and increased running trim.

In the example shown in Figure 5 there is also a notable (but lower magnitude) hump in maximum wave height during an earlier stage of the acceleration phase (located between 4 and 7 L). Although not the focus of the present study, it was observed for most acceleration cases at both speeds that this hump occurred close to the well-known "hull speed", where the length Froude number is approximately $Fr_L = 0.4$. The range $0.4 < Fr_L < 0.5$ is often referred to as the semi-displacement speed regime, where vessel wavemaking resistance is at its highest.

The non-dimensionalised maximum wave height results are plotted against non-dimensional distance from the start position for all seven different acceleration distances at $Fr_h = 1.17$ in Figures 6 and 7 (results are split across two plots for clarity). Similarly, the results for the higher speed ($Fr_h = 1.75$) are presented in Figures 8 and 9. It is clear from the results in all four figures that the peak in maximum wave height created during the acceleration phase was significantly higher than the steady state case for all acceleration distances. It is also clear in all cases that, once at steady-state speed, it takes approximately 3 to 4 boat lengths until the maximum wave height was approximately equivalent to that at the *stabilised* steady-state speed. This trend remained consistent for both steady-state speeds and all seven acceleration distances investigated in this study. This in itself provides a practical conclusion in regards to experiment design and the minimum duration at constant speed before the wave pattern generated is considered to be steady-state. This supports the findings of Calisal (1980) who recommended that a ship model should travel a distance before wave data collection is commenced in order to avoid the effects from the initial acceleration waves.

From Figures 6 to 9 it appears that acceleration distance can influence the magnitude of the peak in maximum wave height that occurs during acceleration (for both constant speed cases). This observation was confirmed by Figure 10, which shows the percentage of increase in maximum wave height plotted as a function of non-dimensional acceleration distance for both steady-state depth Froude numbers of 1.17 and 1.75. The most salient point from this figure is that there is a notable increase in maximum wave height for all acceleration distances at both speeds: with increases ranging from 15% to approximately 40%, with most around 30% to 40%. As can be seen, for the slower of these two speeds ($Fr_h = 1.17$) there is a gradual increase in maximum wave height as acceleration distance increases from 2 to 8 L, after which further increase in acceleration distance has little effect on the increase in maximum wave height. The trend is less clear for the higher speed ($Fr_h = 1.75$), however the increase in maximum wave height was consistently around 50% to 65% for all acceleration distances.

As discussed in the "Wave Wake Issues" section, both the height and period of the generated waves were of equal importance. The corresponding period for each of the maximum waves for each acceleration distance were also quantified, with model scale results summarised in Figure 11. As was the case for the height of the maximum wave, the

period of the maximum wave also clearly showed a notable increase during the acceleration phase over that of the steady-state case (see Figure 12). All acceleration distances for both steady-state speeds resulted in an increase in wave period of approximately 20% to 30%, with the larger increases occurring at the longer acceleration distances.

The increase in both wave height and period during the acceleration phase will likely also result in an increase in wave impact, due to the subsequent increase in wave energy flux. As a result, it is almost certain that higher and potentially more damaging waves are created as a vessel accelerates to a super-critical speed (in finite water depths) than is the case when the same vessel operates at a constant super-critical speed. There also appears to be little practical means of avoiding this outcome, however the level of increase can be limited somewhat, generally by minimising the distance over which the vessel is accelerated, as recommended by PIANC (2003).

Similar to the acceleration cases, our investigation into the effect of deceleration on wave characteristics consists of the same model, two steady-state speeds and seven different distances (refer Table 3 for details). To help describe the analysis process, one of these cases is presented in Figure 13, where the non-dimensionalised maximum wave height at multiple locations from the point at which deceleration commences until after the model has come to rest are plotted as a function of the distance from the point at which deceleration commenced. Similar to Figure 5, the dashed blue curve in Figure 13 show the model speed at a constant value of Fr_h = 1.17 before decreasing to rest over the distance of 10 boat lengths (the deceleration is constant while the velocity decreases linearly and the model position is quadratic in time). The experimental points (orange triangles) indicate the non-dimensionalised maximum wave height at multiple locations along this deceleration distance and beyond. The maximum wave height for the steady-state speed is represented by the dashed red horizontal line.

Unlike the acceleration cases, for which the maximum wave height clearly exceeded that of the steady-state super-critical speed at all acceleration distances investigated, this does not occur in the deceleration example shown in Figure 13 where maximum wave height gradually decreases as distance from the deceleration starting position increases. A similar result is found for all deceleration distances investigated for the speed of Fr_h = 1.17, as can be seen in Figure 14, where most cases there is generally a roughly linear decrease in wave height over distance from the point at which deceleration commenced. In all cases the waves propagate beyond the ship model once at rest. Interestingly, for the higher speed (Fr_h = 1.75, Figure 15) maximum wave height remains approximately equal with the steady-state value for several boat lengths for the slower deceleration cases before gradually decreasing. It is believed this is due to the greater period of time that the model has to transition through the trans-critical speeds when reducing from this higher speed, compared to the lower speed which would have almost immediately entered the trans-critical zone upon commencement

of deceleration. This tends to agree with the findings of Torsvik and Dysthe (2006), who suggested larger soliton (leading) waves were always be generated when decelerating through the critical speed with longer transition times, although here we see the height of the maximum wave in the entire wake has generally not increased beyond that generated at the preceding constant speed. It is also noted that the vessel studied by Torsvik and Dysthe operated in a shallow channel, whereas the present study, we only considered a shallow, but unbounded, waterway.

Analysis of the period of the maximum waves during the deceleration phase at each initial speed also confirmed that the waves did not exceed the corresponding values while at steady-state speed. These results were significant because no published data have been published showing an attempt to quantify transient effects on the characteristics of the highest waves generated by a vessel decelerating through the trans-critical regime.

CONCLUSIONS

This article presents descriptions of model scale experiments performed in a shallow water basin to investigate the characteristics of the waves generated by a vessel travelling in accord with a variable depth Froude number. The height and period of the maximum wave created while either accelerating or decelerating through the trans-critical depth Froude regime (in water of constant depth and infinite width) have been compared against those for the same vessel operating at a constant super-critical speed. It was found that transient effects occur during acceleration that cause an increase in both the height and period of the maximum wave, which will lead to an increase in wave impact, compared to that of the same vessel operating at constant speed and finite water depth. This increase occurred at both super-critical speeds investigated and for each of seven acceleration rates which covered a realistic range (from 2 to 14 ship lengths). It was previously thought that the generation of excessive waves during acceleration could be minimised through rapid acceleration through the trans-critical zone, which was found to be generally supported, but the reduction was relatively modest. Interestingly, no such increase in wave characteristics was observed when the same vessel decelerates back through the trans-critical speed zone. There were however, indications that the waves were depth-affected as speed approached the critical depth Froude number.

The systematic experimental campaign was also useful to inform the model test community about the effects when accelerating a model within a finite water test facility. For example, regardless of the acceleration rate, it took a distance of approximately 3 to 4 boat lengths after the model had achieved the desired steady-state speed before the wave pattern had sufficiently stabilised such that it closely resembled the steady-state case.

ACKNOWLEDGEMENT

The authors acknowledge the support of the Australian Research Council via the Linkage Project LP150100502. They also thank the AMC technical support team for their valuable assistance preparing the experiments.

NOTATION

Fr_h	=	Depth Froude number
Fr_L	=	Length Froude number
g	=	Gravitational constant (m/s^2)
h	=	Water depth (m)
H_m	=	Height of maximum wave (m)
L	=	Length of vessel / ship model (m)
T_m	=	Period of maximum wave (s)
u	=	Model velocity (m/s)

REFERENCES

Akylas, T. R., Kung, T. J., and Hall, R. E. (1988). "Nonlinear groups in ship wakes," *Proc. 17th Symposium in Naval Hydrodynamics*, The Hague, The Netherlands, August 29–September 2, National Academy Press, Washington, D.C.

Austin, I. (1999). "High-speed vessels and their impacts on wetlands and habitat: a case study from San Francisco." In *Proc., Fifth International Conference on Fast Sea Transportation: FAST '99, Seattle, Washington, USA, August 31 - September 2, 1999, The Society of Naval Architects and Marine Engineers (SNAME).*.

Calisal, S. M. (1977). "Effect of initial acceleration of ship wave pattern and wave survey methods." *J. Ship Research*, 21(4), 239-247.

Calisal, S. M. (1980). "Some experimental results with ship model acceleration waves." United States Naval Academy, Division of Engineering and Weapons, Annapolis, Maryland, Report USNA-EW-4-80.

Ertekin, R.C., Webster, W.C. and Wehausen, J.V. (1984). "Ship generated solitons." *Proc. 15th Symp. Naval Hydrodynamics*, Hamburg, 347-364.

Ertekin, R. C., Webster, W. C. and Wehausen, J. V. (1986). "Waves caused by a moving disturbance in a shallow channel of finite width." *J. Fluid Mech*. 169, 275–292.

Feldtmann, M. and Garner, J. (1999). "Seabed modifications to prevent wake wash from fast ferries." *Proc. RINA Int. Conf. on Coastal Ships and Inland Waterways*, London, 17-18 February.

Grue, J. (2017). "Ship generated mini-tsunamis." *J. Fluid Mechanics*, 816, 142-166. doi:10.1017/jfm.2017.67.

International Towing Tank Conference (ITTC).(2014). Recommended Procedure 7.5-02-02-01 Resistance Test.

Lee, S. J., and Grimshaw, R. H. J. (1990). “Upstream-advancing waves generated by three-dimensional moving disturbances,” *Phys. Fluids A*, 2, pp.194–201.

Macfarlane, G.J., Bose, N. and Duffy, J.T. (2014). “Wave wake: focus on vessel operations within sheltered waterways.” *Journal of Ship Production and Design*, 30(3), August.

Macfarlane, G.J., Cox, G. and Bradbury, J. (2008). “Bank erosion from small craft wave wake in sheltered waterways.” *RINA Transactions, Intl. Journal of Small Craft Technology*, Part B, Vol. 150, Issue B2, pp33-48.

Marine Accident Investigation Branch (MAIB). (2000). “Report on the investigation of the man overboard fatality from the angling boat "Purdy" at Shipwash Bank, off Harwich on 17 July 1999.” MAIB Report 1/10/194, 23.

Murphy, J., Morgan, G. and Power, O. (2006). “Literature review on the impacts of boat wash on the heritage of Irelands inland waterways.” University College Cork, Hydraulics and Maritime Research Centre, Aquatic Services Unit and Moore Marine Services Ltd.

Parnell, K.E. and Kofoed-Hansen, H. (2001). “Wakes from large high-speed ferries in confined coastal waters: management approaches with examples from New Zealand and Denmark.” *Journal of Coastal Management*, 29, 217-237.

Parnell, K.E., McDonald, S.C. and Burke, A. (2007). “Shoreline effects of vessel wakes.” *Journal of Coastal Research*, 50.

Permanent International Association of Navigation Congresses (PIANC). (2003). “Guidelines for managing wake wash from high-speed vessels.” Report of Working Group 41, Maritime Navigation Commission, Brussels.

Soomere, T. (2005). “Fast ferry traffic as a qualitatively new forcing factor of environmental processes in non-tidal sea areas: a case study in Tallinn Bay, Baltic Sea.” *Environmental Fluid Mechanics*, vol. 5.

Soomere, T. (2007). “Nonlinear components of ship wake waves”, *ASME Transactions*, vol. 60., pp.120-138.

Strom, K. and Ziegler, F. (1998). “Environmental impacts of wake wash from high speed ferries in the Archipelago of Goteborg.” Environmental Office, Goteborg (in Swedish).

Stumbo, S., K. Fox, F. Dvorak, and L. Elliot. 1999. “The prediction, measurement and analysis of wake wash from marine vessels.” Mar. Technol. 36 (4): 248–260.

Thomson, W. (Lord Kelvin). (1887). “On ship waves.” *Proc. of the Institute of Mechanical Engineers,* 409-433.

Torsvik, T., Dysthe, K., and Pedersen, G. (2006). “Influence of variable Froude number on waves generated by ships in shallow water.” *Physics of Fluids*, 18.

The Vancouver Sun, (2009), “B.C. fast ferries’ voyage to oblivion leads to Middle East.” July 30, 2009.

Wehausen, J.V. (1964). “Effects of initial acceleration upon the wave resistance of ship models.” *Berkeley, CA: Univ. of California, Institute of Engineering Research.*

Wu, T. Y. (1987). “Generation of upstream advancing solitons by moving disturbances,” *J. Fluid Mech*., 184, pp. 75–99.

Table 1. Principal Particulars of Model AMC 00-01

Principal Particular	***Value***
Length overall	1.102 m
Length waterline	1.000 m
Beam waterline	0.337 m
Displacement	10.550 kg
Draught	0.089 m
Area: Station 6	0.06885 m^2
Area: Station 6 below design waterline	0.01434 m^2

Table 2. Acceleration Test Condition Summary

STEADY SPEED	Fr_h = 1.17 u = 2.0 m/s		STEADY SPEED	Fr_h = 1.75 u = 3.0 m/s	
Accel. Rate (m/s^2)	Time to Accel. (s)	Distance to Accel. (m)	Accel. Rate (m/s^2)	Time to Accel. (s)	Distance to Accel. (m)
1.00	2.00	2	2.25	1.33	2
0.50	4.00	4	1.13	2.65	4
0.33	6.00	8	0.75	4.00	6
0.25	8.00	8	0.56	5.36	8
0.20	10.00	10	0.45	6.67	10
0.17	12.00	12	0.38	7.89	12
0.14	14.00	14	0.32	9.38	14

Table 3. Deceleration Test Condition Summary

STEADY SPEED	Fr_h = 1.17 u = 2.0 m/s		STEADY SPEED	Fr_h = 1.75 u = 3.0 m/s	
Decel. Rate (m/s^2)	Time to Decel. (s)	Distance to Decel. (m)	Decel. Rate (m/s^2)	Time to Decel. (s)	Distance to Decel. (m)
-1.00	2.00	2	-2.25	1.33	2
-0.50	4.00	4	-1.13	2.65	4
-0.33	6.00	6	-0.75	4.00	6
-0.25	8.00	8	-0.56	5.36	8
-0.20	10.00	10	-0.45	6.67	10
-0.17	12.00	12	-0.38	7.89	12
-0.14	14.00	14	-0.32	9.38	14

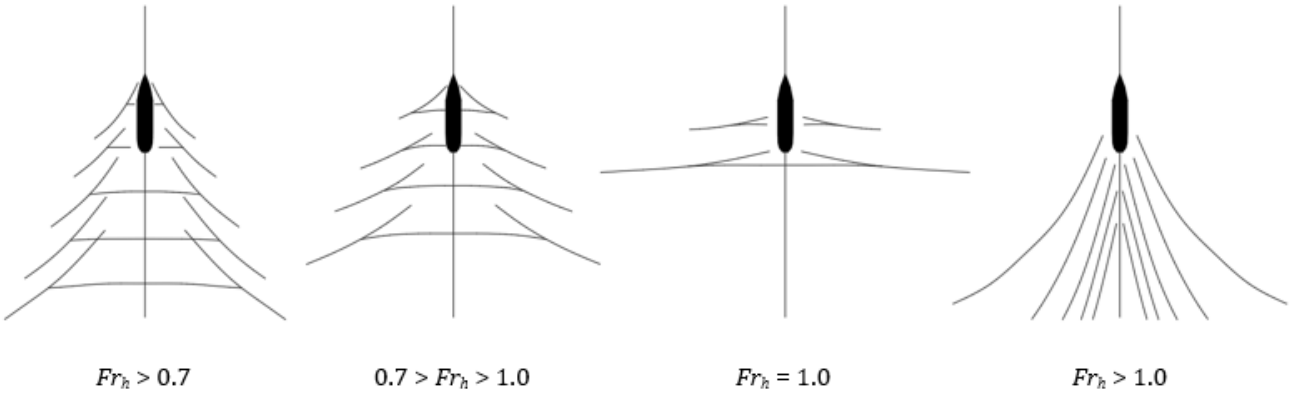

Fig. 1. Vessel wave wake idealised throughout varying Froude depth numbers.

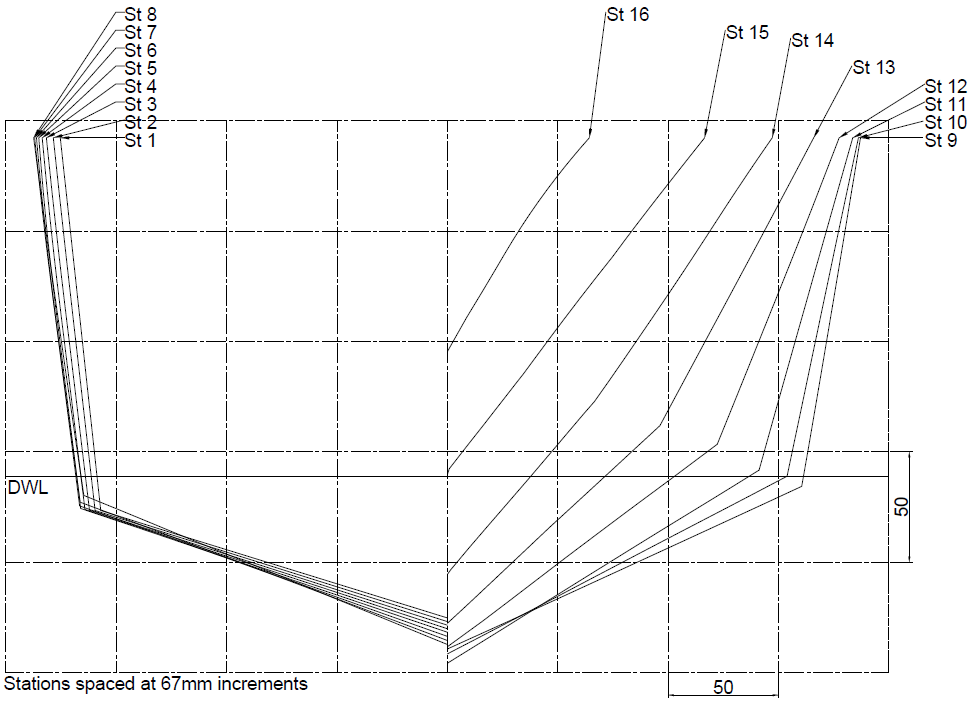

Fig. 2. Body plan of Model AMC 00-01

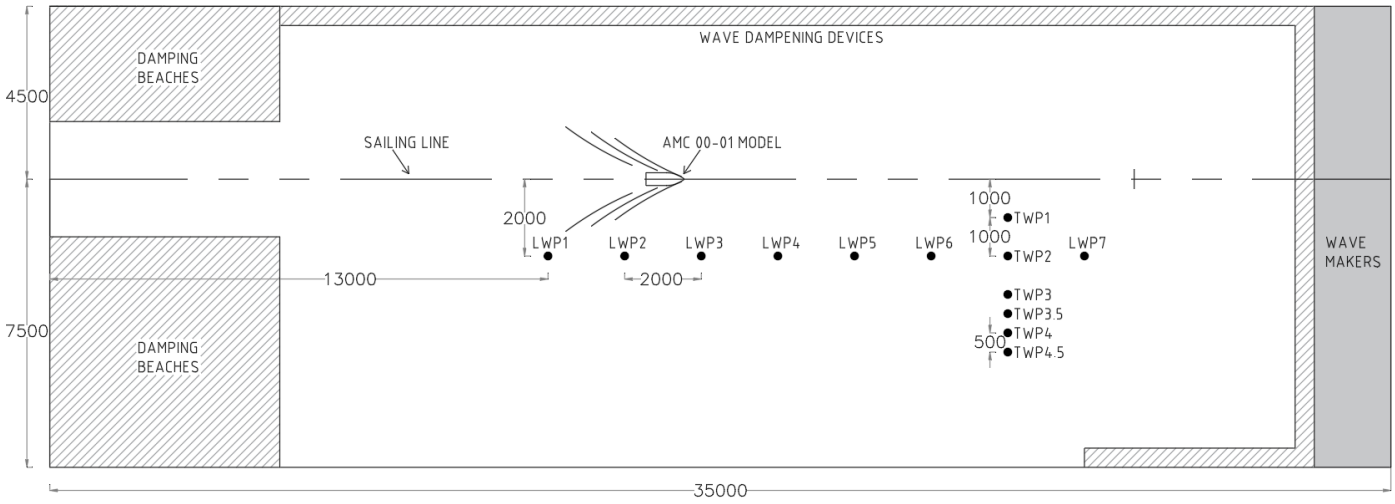

Fig. 3. Plan view of the experimental setup. The longitudinal array of wave probes consists of sensors LWP1 to LWP7 and TWP2.

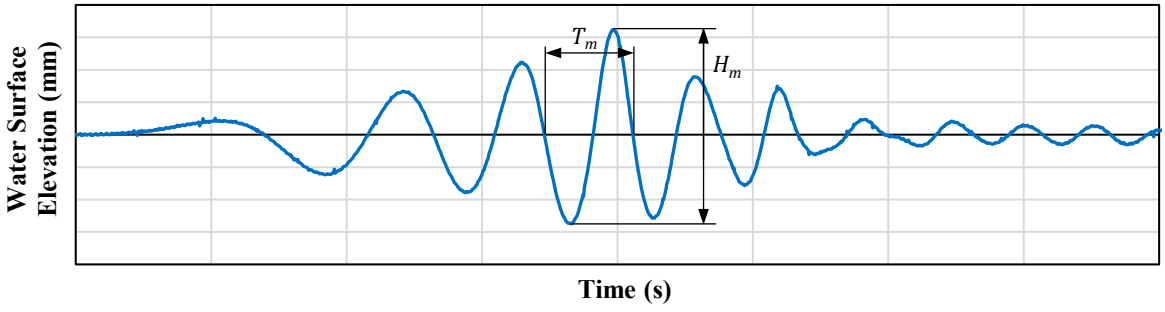

Fig. *4.* Typical water surface elevation time series recorded from a wave probe.

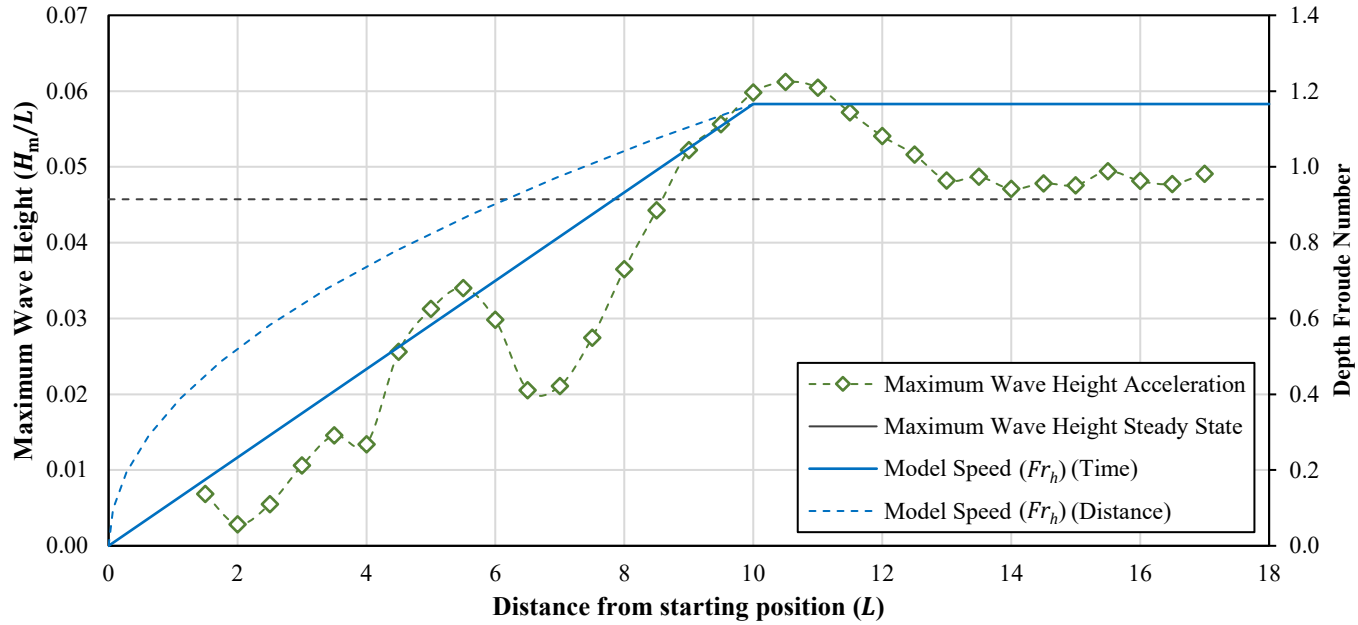

Fig. 5. Sample plot of non-dimensional maximum wave height as a function of distance from starting position for an acceleration distance of 10 L and steady speed of Fr_h = 1.17.

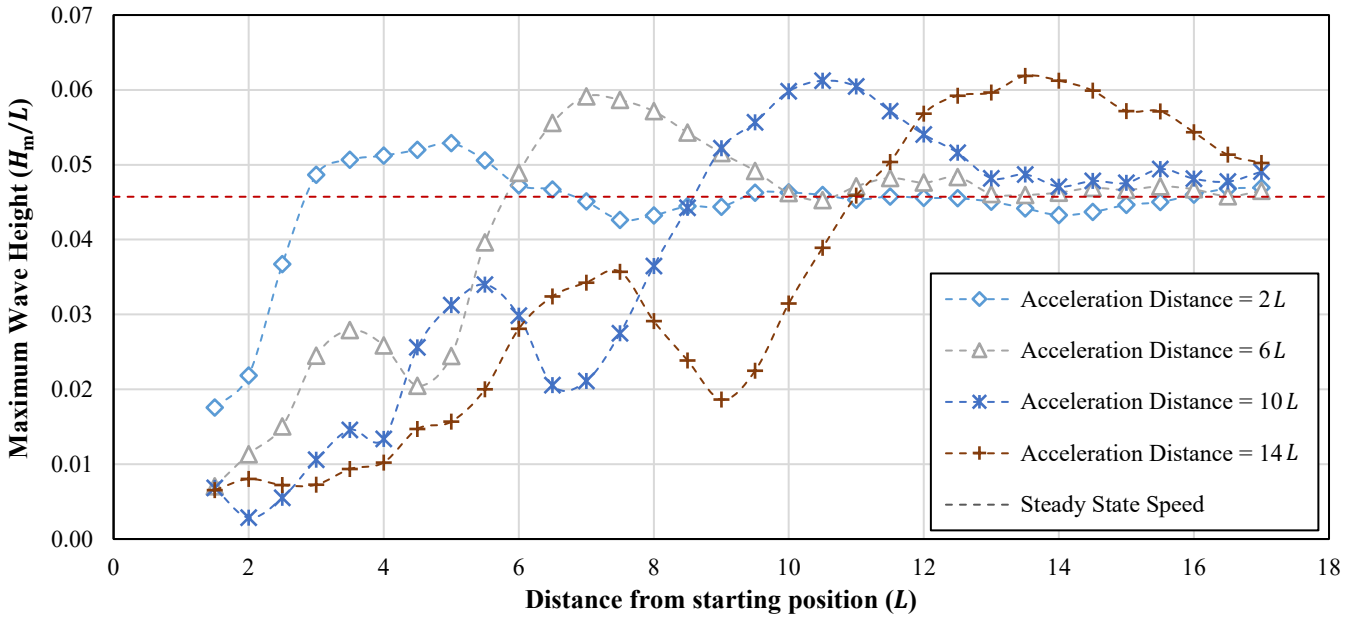

Fig. *6.* Plot of maximum wave heights over distance from starting position for acceleration distances 2, 6, 10, and 14 L at steady state speed of Fr_h = 1.17.

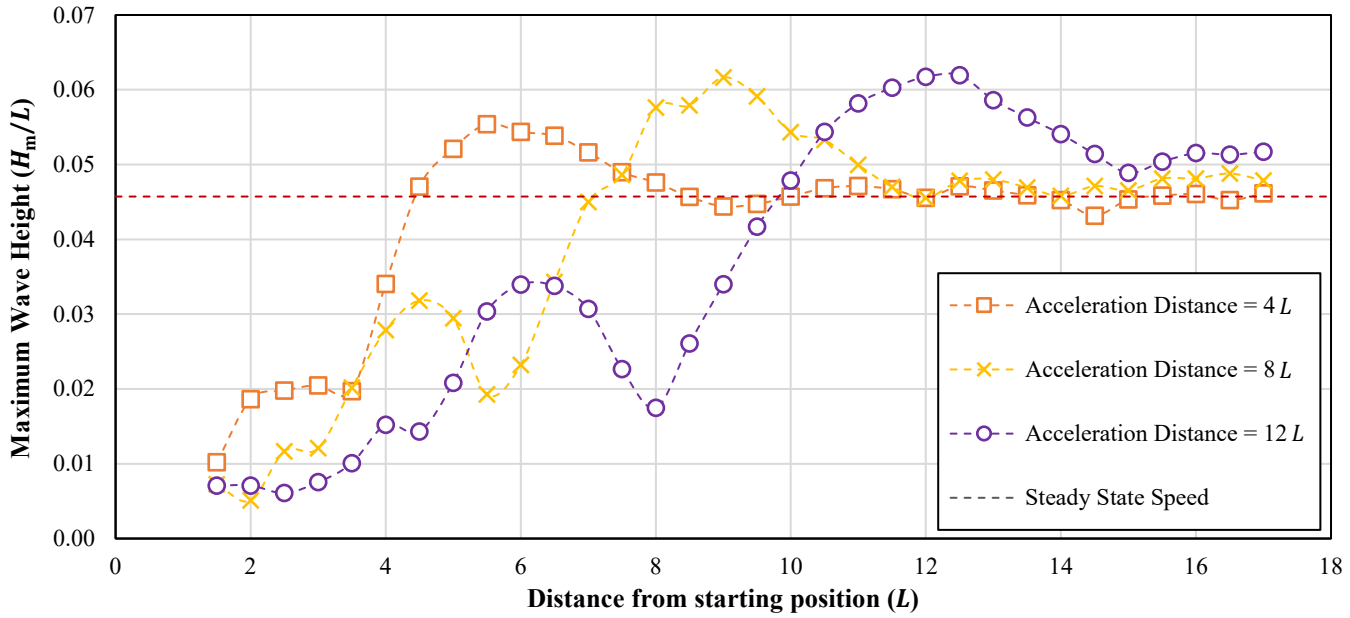

Fig. 7. Plot of maximum wave heights over distance from starting position for acceleration distances 4, 8, and 12 L at steady state speed of Fr_h = 1.17.

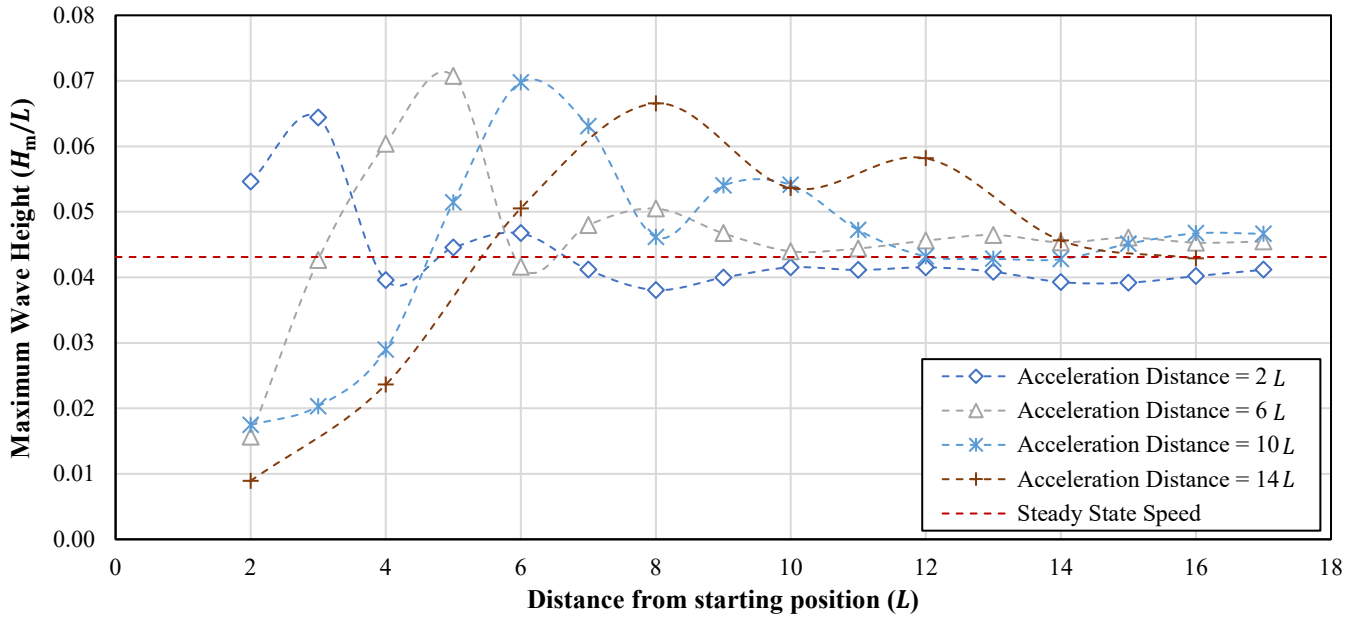

Fig. 8. Plot of maximum wave heights over distance from starting position for acceleration distances 2, 6, 10, and 14 L at steady state speed of Fr_h = 1.75.

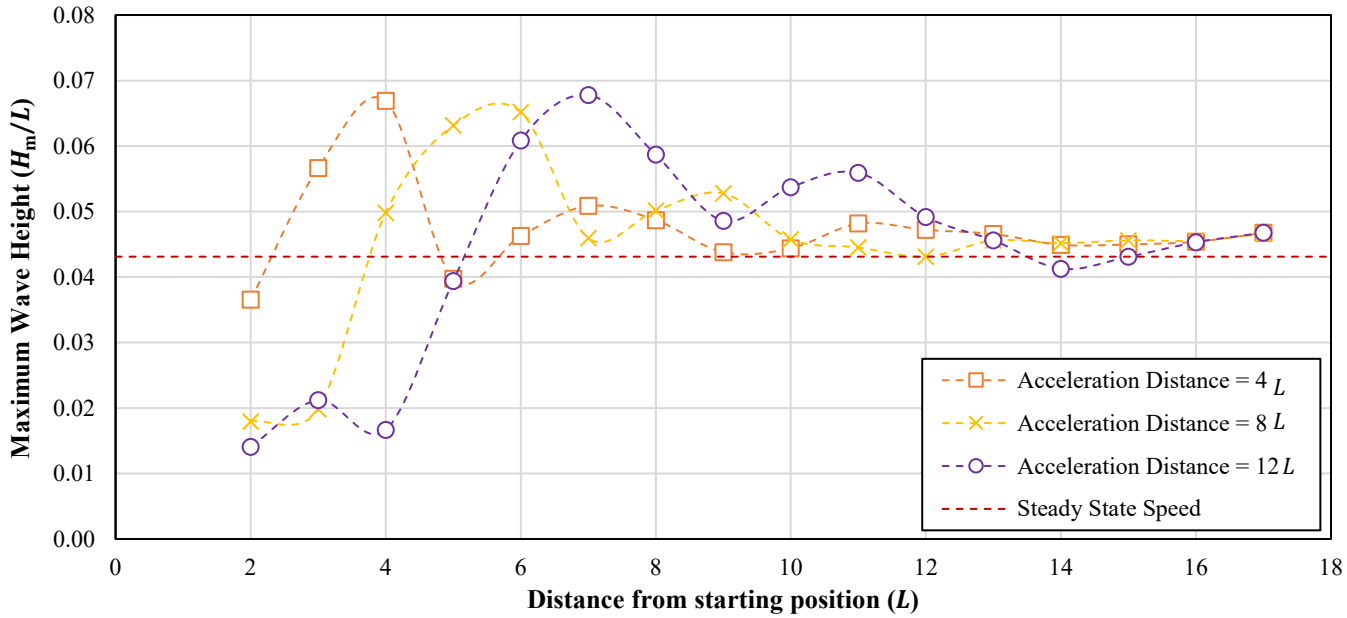

Fig. 9. Plot of maximum wave heights over distance from starting position for acceleration distances 4, 8, and 12 L at steady state speed of Fr_h = 1.75.

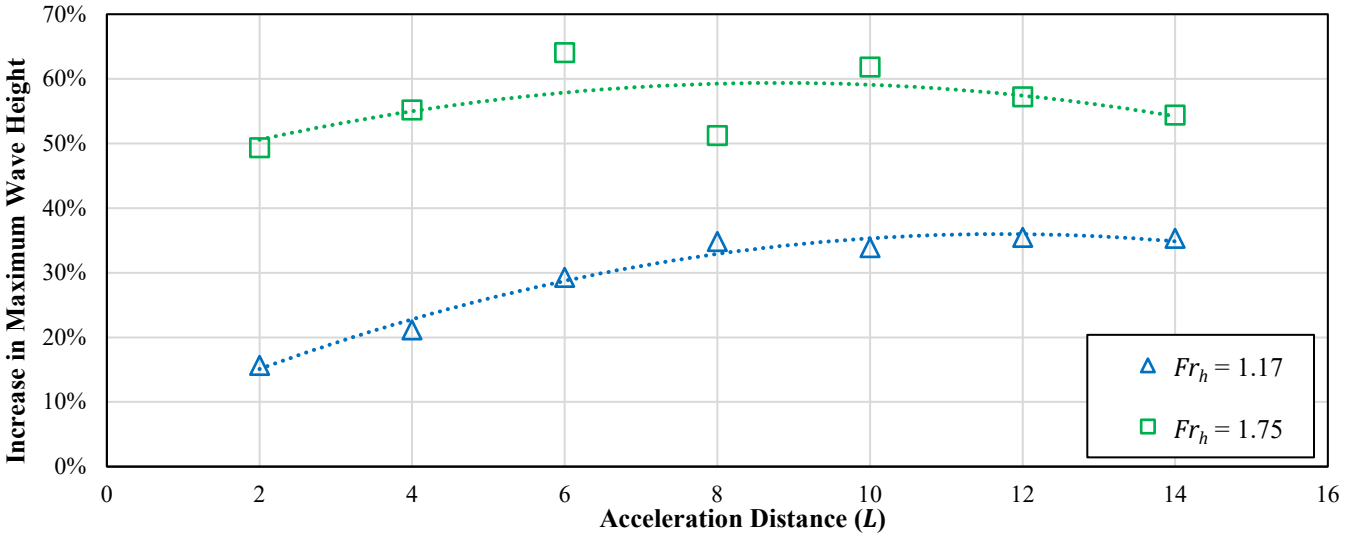

Fig. 10. Plot of increase in maximum wave height as a function of acceleration distance.

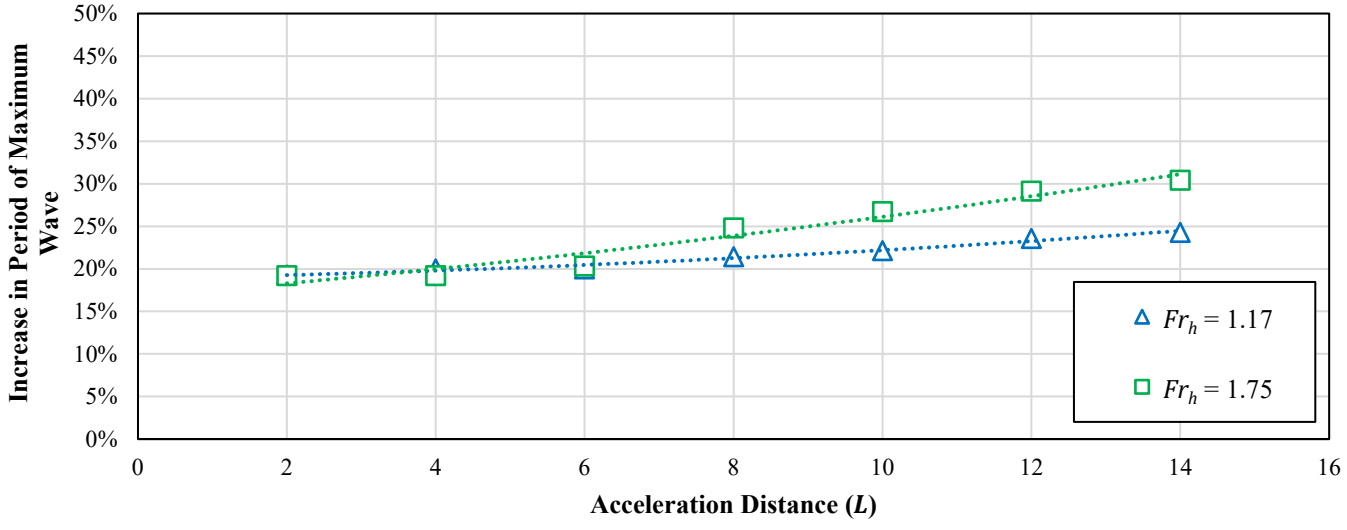

Fig. 11. Plot of periods of the maximum significant waves found in each acceleration case against acceleration distance.

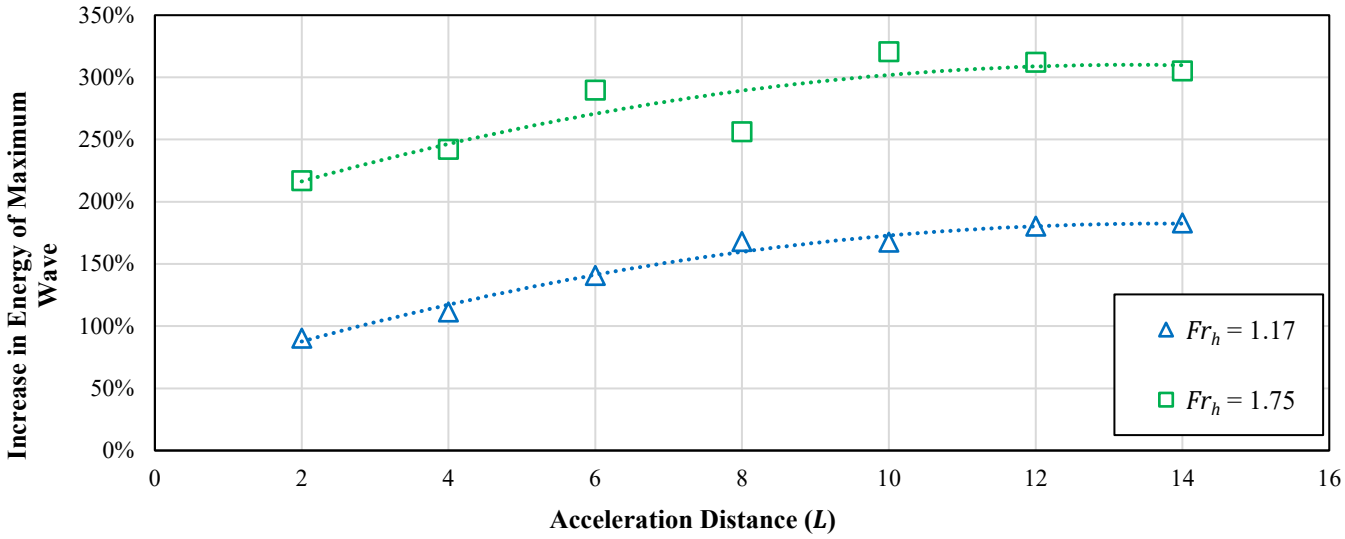

Fig. 12. Plot of wave energy (per unit width of wave crest) against acceleration distance for Fr_h = 1.17 and 1.75 steady state speeds.

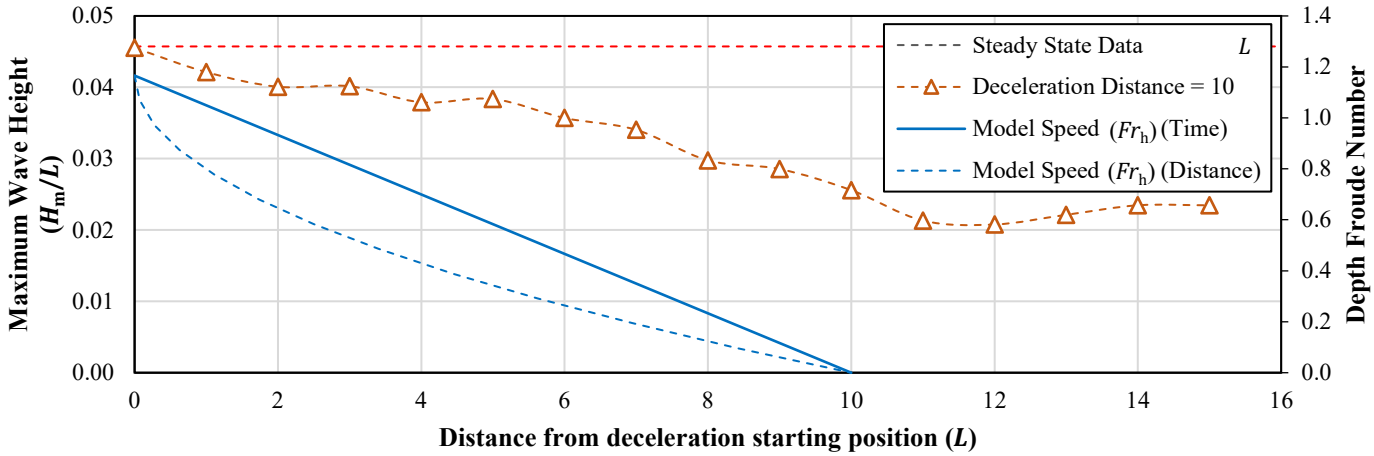

Fig. 13. Sample plot of maximum wave height over distance against distance from deceleration starting position at a deceleration distance of 10 L and steady speed of Fr_h = 1.17.

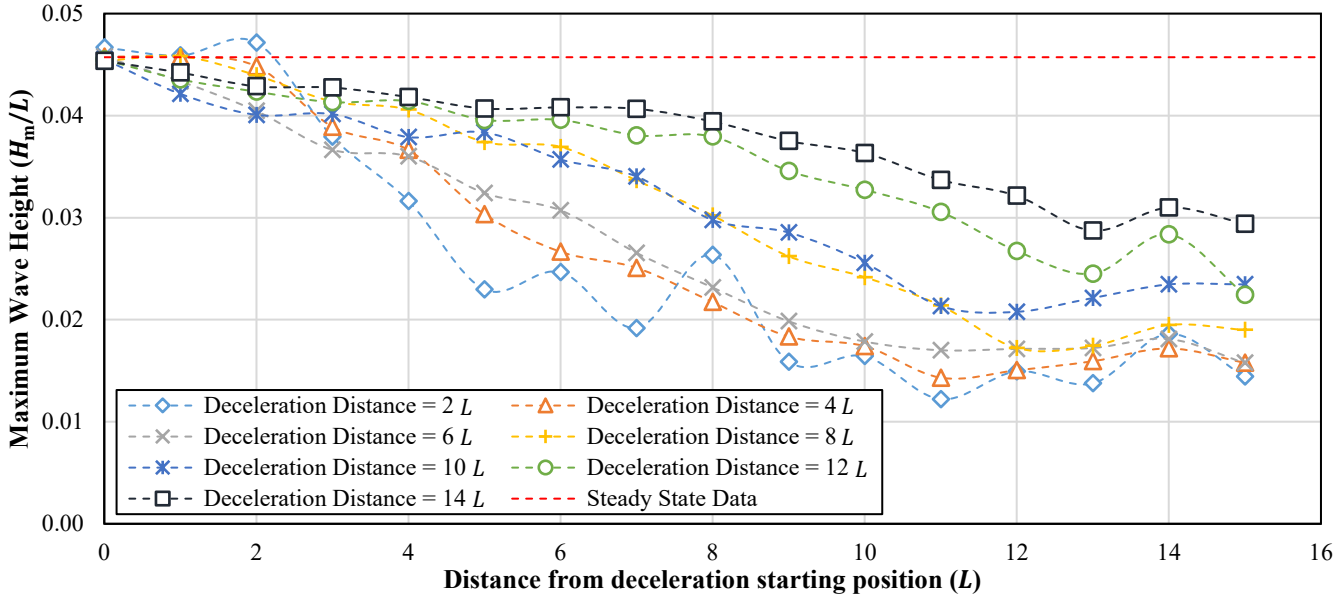

Fig. 14. Plot of maximum wave height as a function of distance from deceleration starting position for different deceleration distances at steady state speed of Fr_h = 1.17.

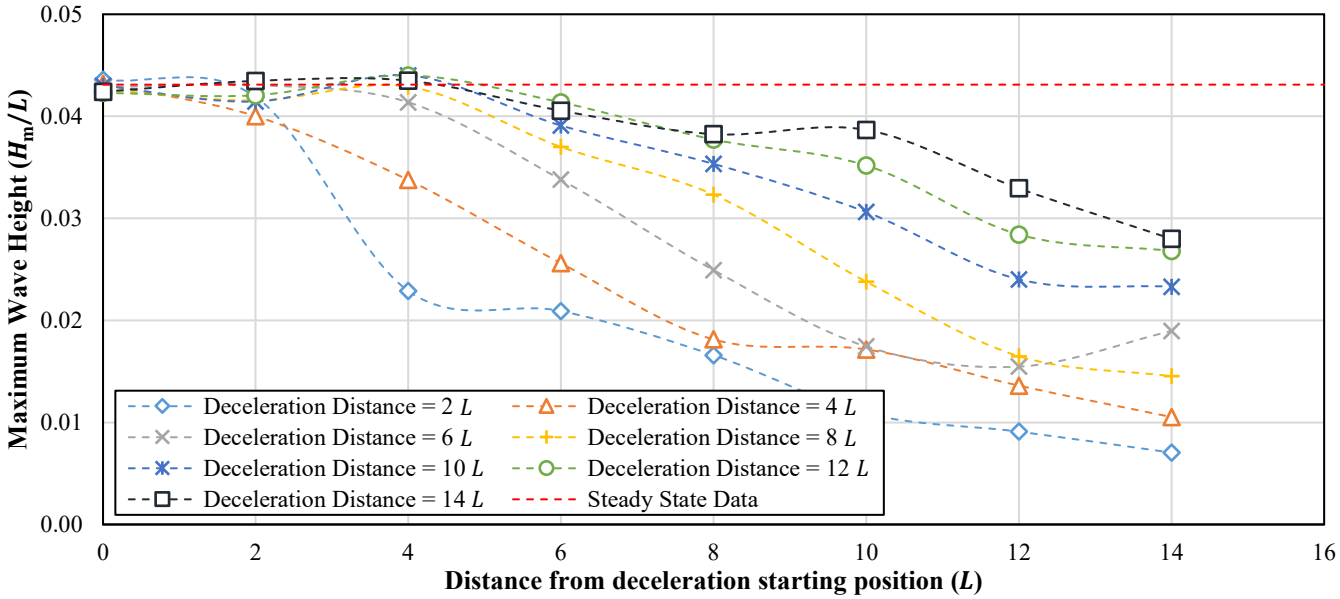

Fig. 15. Plot of maximum wave height as a function of distance from deceleration starting position for different deceleration distances at steady state speed of Fr_h = 1.75.